

X-Ray Spectroscopy of the Classical Nova V458 Vulpeculae with Suzaku

Masahiro TSUJIMOTO,^{1,2*} Dai TAKEI,³ Jeremy J. DRAKE,⁴ Jan-Uwe NESS,^{5†} and Shunji KITAMOTO³

¹*Department of Astronomy & Astrophysics, Pennsylvania State University,
525 Davey Laboratory, University Park, PA 16802, USA*

²*Japan Aerospace Exploration Agency, Institute of Space and Astronautical Science,
3-1-1 Yoshino-dai, Sagami-hara, Kanagawa 229-8510*

³*Department of Physics, Rikkyo University, 3-34-1 Nishi-Ikebukuro, Toshima, Tokyo 171-8501*

⁴*Smithsonian Astrophysical Observatory, MS-3, 60 Garden Street, Cambridge, MA 02138, USA*

⁵*School of Earth and Space Exploration, Arizona State University, Tempe, AZ 85287, USA
tsujimot@astro.isas.jaxa.jp*

(Received 2018 October 29; accepted 2018 October 29)

Abstract

We conducted a target of opportunity X-ray observation of the classical nova V458 Vulpeculae 88 days after the explosion using the Suzaku satellite. With a ~ 20 ks exposure, the X-ray Imaging Spectrometer detected X-ray emission significantly harder than typical super-soft source emission. The X-ray spectrum shows $K\alpha$ lines from N, Ne, Mg, Si, and S, and L-series emission from Fe in highly ionized states. The spectrum can be described by a single temperature (~ 0.64 keV) thin thermal plasma model in collisional equilibrium with a hydrogen-equivalent extinction column density of $\sim 3 \times 10^{21}$ cm $^{-2}$, a flux of $\sim 10^{-12}$ erg s $^{-1}$ cm $^{-2}$, and a luminosity of $\sim 6 \times 10^{34}$ erg s $^{-1}$ in the 0.3–3.0 keV band at an assumed distance of 13 kpc. We found a hint of an enhancement of N and deficiencies of O and Fe relative to other metals. The observed X-ray properties can be interpreted as the emission arising from shocks of ejecta from an ONe-type nova.

Key words: stars: individual (Nova Vulpeculae 2007 number 1, V458 Vulpeculae) — stars: novae — X-rays: stars

1. Introduction

Classical novae occur in accreting binaries with a white dwarf (WD) as the primary. Hydrogen-rich accreted material is accumulated on the WD surface until a critical mass is reached that ignites a thermonuclear runaway. A wind driven by radiation pressure leads to ejection of accreted and partially nuclear-processed material, forming an optically thick shell around the binary system. The nova terminates once the remaining hydrogen is consumed on the WD surface. Reviews of classical novae can be found in e.g., Gehrz et al. (1998); Starrfield et al. (2008).

Classical novae are copious X-ray emitters (e.g., Krautter 2002). Several processes are involved in producing the X-rays. One is photospheric emission from a hot layer of the WD surface fueled by residual nuclear burning after the explosion. The layer is rendered visible after the ejecta shell expands and becomes less opaque to soft X-rays. Its X-ray spectrum is characterized by a very soft blackbody-like emission with a temperature of $\lesssim 50$ eV and is easily identified in medium-resolution CCD spectra. Higher-resolution grating spectroscopy can further identify absorption features by the WD atmosphere over the blackbody continuum (Ness et al. 2003). These types of X-ray emitters are known as super-soft sources

(SSS).

Another type of X-ray emission originates from circumstellar material that is photoionized by the SSS emission. This reprocessed emission is usually dwarfed by the ionizing source. However, when the surface nuclear fuel is consumed and the SSS emission fades out, residual emission from the heated surrounding medium can emerge. This was found in the nova V382 Vel, in which the residual emission was interpreted as the radiatively cooling ejecta that are optically thin and have reached a collisional equilibrium (Ness et al. 2005). Similar line-dominated emission was found in V4743 Sgr, when the SSS emission turned off for a brief period for unknown reasons (Ness et al. 2003).

Yet another type is weak and hard X-rays, which a substantial fraction of X-ray-emitting novae exhibit within a year of the outburst before the SSS emission becomes visible. In systematic studies by ROSAT (Orio et al. 2001) and Swift (Ness et al. 2007), more than half and six out of eight are among such novae, respectively. While their spectra are similar to that found in V382 Vel (Ness et al. 2005), their origin is probably different; the ejected material has not expanded enough to be optically thin, and no ionizing source is present to heat up the surrounding material. Several possible origins have been proposed for the hard X-rays including shock heating of expanding ejecta (Lloyd et al. 1992; O’Brien et al. 1994) and reestablished accretion. The latter explains the X-rays seen in a nova

* Chandra Fellow

† Chandra Fellow

by a magnetic WD (V2487 Oph; Hernanz & Sala 2002).

Detailed and timely spectroscopy is requisite to understanding the origin of the early hard X-ray emission, but it is complicated by the faint and more transient nature of this phenomenon. While grating spectroscopy yields a wealth of information, it is limited to extremely bright sources. Only two novae have been studied with grating spectroscopy for their hard emission, but they are atypical samples; RS Oph (Nelson et al. 2008; Drake et al. 2008a; Ness et al. 2008a) is a symbiotic nova, where shocks are expected between the expanding ejecta and the stellar wind of the giant companion. Hard emission from V382 Vel (Ness et al. 2005) was also observed with grating, but the emission has a different origin as described earlier. Hard emission in most classical novae with a main sequence companion has generally been studied based on scant low-resolution spectra and data of poor statistical quality. The utility of such data is limited to determination of the plasma temperature and X-ray extinction from broad-band spectral shapes. Few studies to date attempted to go beyond this (Mukai & Ishida 2001; Orio et al. 2001; Hernanz & Sala 2007).

Suzaku fills the gap well. Its medium-resolution CCD spectrometer yields a high signal-to-noise ratio spectrum for moderately bright X-ray sources in a reasonable telescope time. It has sufficient spectral resolution to resolve emission lines from abundant elements. While we can only rely on global spectral models, the relative flux and energy of these lines enable us to conduct a temperature diagnosis, to study the plasma evolution using non-equilibrium features in emission lines, and to reveal abundance patterns in the X-ray-emitting plasma.

Here, we present a Suzaku spectroscopic study of the nova V458 Vulpeculae (V458 Vul) 88 days after the explosion. A high signal-to-noise ratio spectrum of the hard X-ray emission was obtained using the X-ray Imaging Spectrometer (XIS). Emission lines from highly-ionized N, Ne, Mg, Si, S, and Fe are resolved, enabling us to conduct the types of diagnosis described above. We present the finding of the study and discuss their implications.

2. V458 Vulpeculae

2.1. Ground-based monitoring

On 2007 August 8.54 UT, an optical nova reaching a visual magnitude of ~ 9.5 mag was spotted in the constellation Vulpecula at (RA, Dec) = ($19^{\text{h}}54^{\text{m}}24^{\text{s}}.66$, $+20^{\circ}52'51''.7$) in the equinox J2000.0 (Nakano et al. 2007). The variable star was fainter by ~ 8 mag before the explosion if a cataloged source (USNO-A2.0 1050-15545600; Monet et al. 1998) is its precursor. Optical spectroscopic observations on the following day revealed hydrogen and helium emission lines with P-Cygni profiles with a full width at half maximum (FWHM) of $1750\text{--}1900\text{ km s}^{-1}$ (Buil & Fujii 2007), establishing the classical nova nature of this source. The nova was named V458 Vul (Samus 2007).

Subsequent ground-based observations were made both photometrically and spectroscopically. The light curve

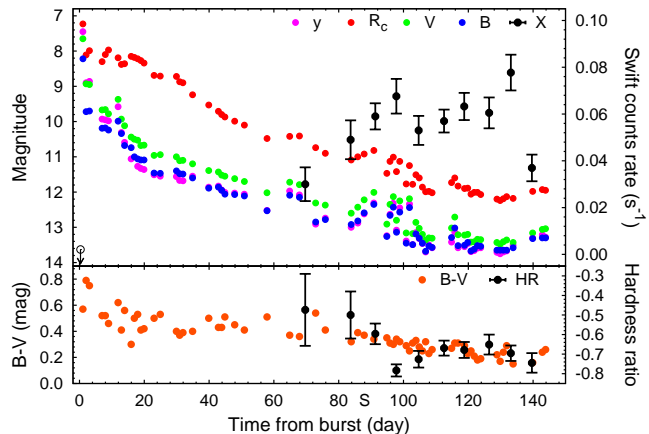


Fig. 1. Evolution of V458 Vul in brightness and color (upper and lower panels, respectively). The origin of the abscissa is day 54320.54 in modified Julian date when the nova was first spotted (Nakano et al. 2007). The epoch of the Suzaku observation is indicated with “S” on the abscissa. In the upper panel, the y -, R_c -, V -, and B -band magnitudes (private communication with K. Nakajima) are respectively shown in magenta, red, green, and blue, while the Swift X-ray count rate (0.3–10.0 keV) is shown in black with 1σ errors (Ness et al. 2008b). The 95.5% upper-limit for non-detected X-rays on day 1 is indicated by an open circle. In the lower panel, the $B-V$ color is shown in orange, while the Swift hardness ratio is in black with 1σ errors. Hardness ratio is defined by $(H-S)/(H+S)$, where S and H are the Swift count rates in the 0.25–1.5 keV and 1.5–10 keV band, respectively.

of the nova (Bianciardi et al. 2007a; Bianciardi et al. 2007b; Broens et al. 2007; Casas et al. 2007; Labordena et al. 2007; Nakamura et al. 2007; Scarmato 2007) declined from the maximum V -band magnitude of 7.65 mag on day 1.42 to ~ 14 mag in five months with time scales of $t_2 \sim 7$ day (Poggiani 2008), where t_2 is the time of decline from the optical maximum by 2 mag. The declining trend is globally monotonic, but with several exceptions of local brightening at around 68 and 95 days after the explosion (figure 1). The earliest spectra (Kiss & Sarneczky 2007; Lynch et al. 2007; Munari et al. 2007; Prater et al. 2007; Skoda et al. 2007; Tarasova 2007) are characterized by P Cygni profiles in H Balmer series, He I, and Fe II lines. From all these data, the nova was initially classified as a very fast (Payne-Gaposchkin 1957) and a Fe II-type (Williams 1992) nova. However, subsequent observations obtained approximately one month after the outburst show that the Fe lines have faded and the N II and N III lines have gained prominence, indicating an evolution toward a He/N class nova (Poggiani 2008). Wesson et al. 2008 found that this nova occurred inside a planetary nebula with $H\alpha$ imaging, a second such case after GK Per.

We adopt the distance to V458 Vul to be 13 kpc (Wesson et al. 2008). In a series of $H\alpha$ images taken in May 2008, a bright circumstellar knot was discovered at $3''.5$ away from the central source. By assuming that the knot is illuminated by the flash of the nova, the distance of ~ 13 kpc was derived. This is consistent

with two other distance estimates. The one is derived from a maximum-magnitude versus rate-of-decline relation (Downes & Duerbeck 2000), an empirical relation that intrinsically bright novae fade our fast. The other is derived from the assumption that the measured radial velocity stems only from the Galactic rotation (Wesson et al. 2008).

The interstellar extinction ($A_{V,ISM}$) was estimated to be 1.76 ± 0.32 mag (Poggiani 2008). This converts to an interstellar hydrogen-equivalent extinction column density ($N_{H,ISM}$) of $3.15 \pm 0.57 \times 10^{21}$ cm $^{-2}$ using the relation $N_{H,ISM}/A_{V,ISM} = 1.79 \times 10^{21}$ cm $^{-2}$ mag $^{-1}$ (Predehl & Schmitt 1995). The line-of-sight extinction integrated through our Galaxy toward V458 Vul is estimated from HI maps to be 3.7×10^{21} cm $^{-2}$ (Kalberla et al. 2005) or 4.0×10^{21} cm $^{-2}$ (Dickey & Lockman 1990), which is consistent that the nova is within in our Galaxy.

2.2. Space-based monitoring

Monitoring observations were also conducted with space-based facilities. The X-Ray Telescope (XRT; Burrows et al. 2005) aboard Swift was employed to take an immediate follow-up image on day 1 and repeated snapshots from day 71 to 140 (figure 1). The X-ray emission was not detected on day 1, but it started to emerge on day 70 during the first optical rebrightening. A total of 192 X-ray counts were accumulated in a short observation of ~ 6.7 ks, which is at least 10 times brighter than the upper limit to the X-ray counts on day 1 (Drake et al. 2007). The X-ray flux continued to increase until the peak on day ~ 100 , showed a stable flux for ~ 30 days, then decreased in flux quite sharply on the last Swift visit on day 140.

The XRT spectrum on day 70 has significant signal above 1 keV, indicating that hard X-ray emission component was present in addition to any soft emission typical of the SSS phase (Drake et al. 2007). No detailed spectroscopy was possible due to the paucity of counts. We therefore requested a director's discretionary time on the Suzaku telescope to obtain an X-ray spectrum of better statistics and resolution. A ~ 20 ks observation was conducted on day 88. We present the detailed analysis of the Suzaku observation in this paper. Swift resumed its observing campaign on day 315. In this later phase, the hard X-ray flux is highly variable and is anti-correlated with the UV flux. The Swift results, including the later observations, are presented in Drake et al. (2008b); Ness et al. (2008b).

3. Observation

Suzaku observed V458 Vul on 2007 November 4 from 7:51 UT to 21:00 UT. The observatory (Mitsuda et al. 2007) carries two instruments: the X-ray Imaging Spectrometer (XIS: Koyama et al. 2007) sensitive at 0.2–12 keV and the Hard X-ray Detector (HXD: Kokubun et al. 2007; Takahashi et al. 2007) at 10–600 keV. We concentrate on the XIS data in this paper, which has sensitivity for the energy range of interest.

The XIS is equipped with four X-ray CCDs. Three of

them (XIS0, 2, and 3) are front-illuminated (FI) devices, while the remaining one (XIS1) is back-illuminated (BI). FI and BI CCDs are superior to each other in the hard and soft band responses, respectively. XIS2 has not been functioning since 2006 November, and we use data from the remaining three devices. The CCDs are mounted at the focus of four independent X-ray telescopes (Serlemitsos et al. 2007), which are aligned to observe a $\sim 18' \times 18'$ field with a half-power diameter of $\sim 2'$.

The three imaging-spectrometers have a combined effective area of ~ 1030 cm 2 at 1.5 keV. We used the spaced-row charge injection technique, which rejuvenates the degraded spectral resolution by filling the charge traps with artificially injected electrons during CCD readouts. This yields an FWHM resolution of 145–174 eV at 5.9 keV.

The observation was conducted using the normal clocking mode with a frame time of 8 s. Data were cleaned using processing version 2.1 to remove non-X-ray events and those taken during the South Atlantic Anomaly passages, at elevation angles below 5° from the Earth rim, and at elevation angles below 20° from sunlit Earth rim. After filtering, the net integration time is ~ 19.6 ks. We used HEASoft version 6.4.1¹ for the data reduction and Xspec version 11.3.2² for the X-ray spectral analysis.

4. Analysis

4.1. Image and Timing

Figure 2 shows the XIS image in the 0.2–5.0 keV band obtained by merging the events recorded by all the three CCDs. Four sources were detected by visual inspection. The brightest one at the center is V458 Vul based on astrometric consistency with the Swift data. We fine-tuned the coordinate of the XIS image using this source as a reference. The resulting positions, X-ray count rates (CR), and hardness ratio (HR) of the four sources are summarized in table 1. None of the sources except for V458 Vul has records in the SIMBAD or the NASA/IPAC Extragalactic Database, leaving their natures unclear.

The background was subtracted to compute CR and HR. Source counts were integrated in circles with adaptively-chosen radii to maximize the ratio against background for all sources (solid circles in figure 2). Background counts were accumulated in a different method for V458 Vul and the others. For V458 Vul, background was from an annular region with inner and outer radii of $5'$ and $7'$, respectively. For the other sources, it was from annuli around V458 Vul with the inner circle circumscribed to and the outer circle inscribed to the source extraction circle of each source. The $3'$ circles around all sources were masked in these annuli. In this way, we canceled the contamination to the faint three sources by the dominantly bright source 1. The background was corrected for the vignetting before subtracting from the source. The contamination of source 1 by source 2 is con-

¹ See <http://heasarc.gsfc.nasa.gov/docs/software/lheasoft/> for detail.

² See <http://heasarc.gsfc.nasa.gov/docs/xanadu/xspec/index.html> for detail.

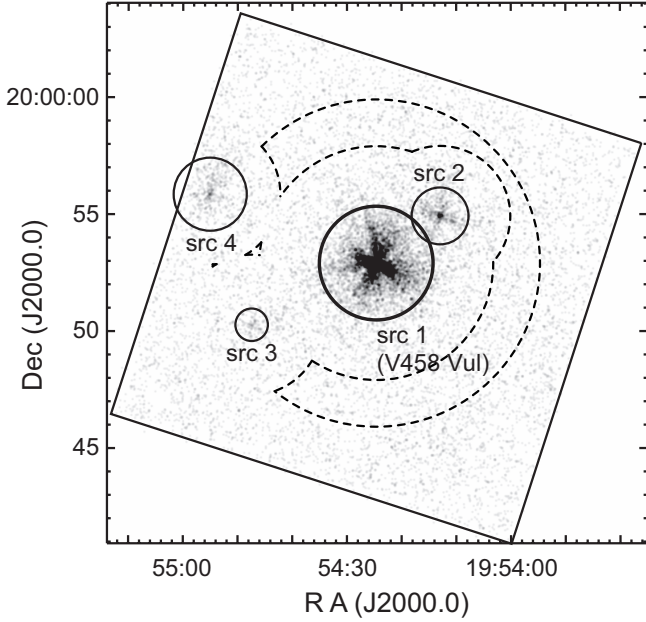


Fig. 2. Smoothed XIS image in the 0.2–5.0 keV band. Three CCD images were merged and a Gaussian smoothing was applied. V458 Vul (source 1) and three faint sources (sources 2–4) were detected. The source regions are shown with solid circles around each source, while the background region for V458 Vul is shown with broken annulus with masks.

Table 1. Source list.

Source	RA (J2000.0)	Dec (J2000.0)	CR* (s ⁻¹)	HR [†]
1 [‡]	19 ^h 54 ^m 25 ^s	+20°52′52″	9.8×10^{-2}	-0.55
2	19 ^h 54 ^m 13 ^s	+20°54′53″	7.9×10^{-3}	+0.43
3	19 ^h 54 ^m 47 ^s	+20°50′13″	2.7×10^{-3}	+0.40
4	19 ^h 54 ^m 55 ^s	+20°55′48″	5.2×10^{-3}	-0.34

* The background-subtracted count rate in the 0.2–5.0 keV averaged over the three CCDs. The values are normalized to the circular aperture of a 3′ radius.

† The hardness ratio defined as (H–S)/(H+S), where H and S are background-subtracted count rates in the hard (1.5–5.0 keV) and soft (0.2–1.5 keV) band, respectively.

‡ V458 Vul. The contamination by source 2 is not corrected in the CR and HR values.

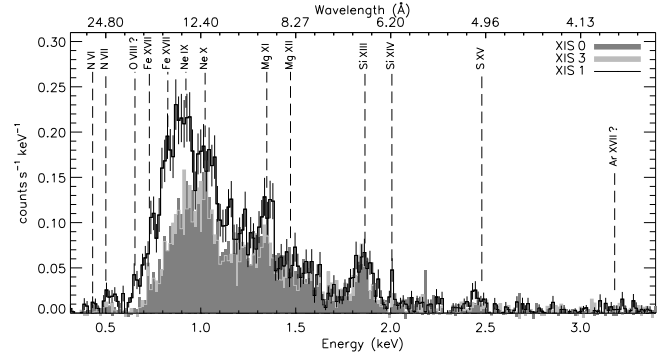


Fig. 3. X-ray spectra of V458 Vul (background subtracted) in a linear scale using the XIS0 and XIS3 (both FI devices; dark and light gray shadings, respectively) and with the XIS1 (BI device; solid line). The energies of plausible emission lines are labeled.

considered later.

We constructed a light curve of V458 Vul and found no significant changes. The curve was fitted with a constant flux model with a null hypothesis probability of 53%.

4.2. Spectrum

Figure 3 shows the background-subtracted XIS spectra of V458 Vul in a linear scale at the 0.4–3.5 keV band. We see conspicuous K α line emission from NVII, Ne IX, Ne X, Mg XI, Mg XII, Si XIII, and S XV. We also see some emission from Fe XVII L-series lines.

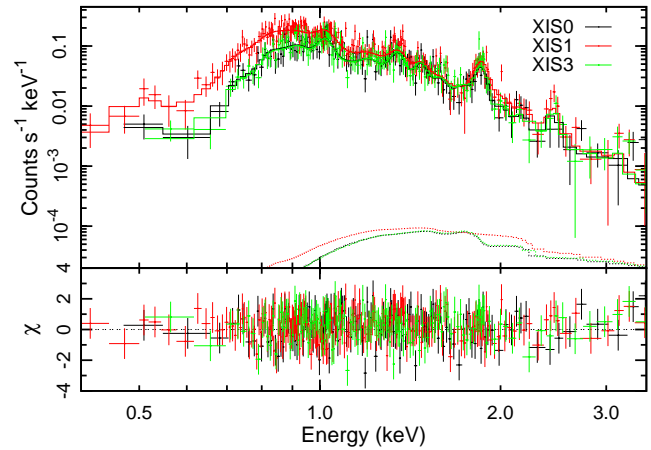


Fig. 4. Best-fit models to the background-subtracted spectra in a logarithmic scale. Different colors are used for each CCD. The top panel shows the data with crosses and the best-fit model with solid lines. The contamination by the nearby source 2 is included as dotted lines. The bottom panel shows the residuals to the fit.

In order to model the spectrum, we generated the redistribution matrix functions and the auxiliary response functions using `xismfgen` and `xissimarfgen` (Ishisaki et al. 2007), respectively. The difference in effective area arising from different off-axis angles between the source and the background regions were compensated following

the procedure described in Hyodo et al. (2008).

The contamination by the nearby source 2 was considered by including an additional absorbed power-law model ($7.8 \times 10^{21} \text{ cm}^{-2}$ for the absorption column and 2.1 for the photon index) that best describes its spectrum. From a ray-tracing simulation, we found that $\sim 1.5\%$ of the emission from source 2 is in the source extraction region of source 1. Fortunately, sources 1 and 2 have different spectral hardness (table 1) and the contamination by source 2 is almost negligible.

We fitted the 0.3–3.0 keV spectrum of source 1 using an optically-thin thermal plasma model in collisional equilibrium (the APEC model; Smith et al. 2001) convolved with an interstellar absorption assuming the cross sections and the chemical abundance in Wilms et al. (2000). The plasma temperature ($k_{\text{B}}T$) and its emission measure as well as the hydrogen column density (N_{H}) were allowed to vary.

For the chemical composition of the plasma, we tried four models with different constraints on the abundance of elements (Model 1–4). The base-line model is the “Model 1”, in which the abundance of elements with noticeable $K\alpha$ emission (N, Ne, Mg, Si, and S) were allowed to vary individually. Also, the abundance of Fe was also varied, as the Fe L series emission is necessary to explain the spectrum between the O VIII $K\alpha$ (0.65 keV) and Ne IX $K\alpha$ (0.92 keV) features. The abundance of Ni, which also contributes through its L series emission, was tied to that of Fe at the solar ratio. Other elements were fixed to the solar abundance. Here, we assumed the solar values by Anders & Grevesse (1989). The spectrum and the best-fit model is shown in figure 4, and the best-fit parameters are summarized in table 2. Additional components are not statistically required to explain the spectra.

For the other models, we put additional constraints on the “Model 1” for the purpose of reducing the statistical uncertainties. In the “Model 2”, we tied the abundance of intermediate-mass elements (Ne, Mg, Si, S) after confirming that the abundance of these elements is consistent with each other in the “Model 1”. In the “Model 3”, we fixed the N abundance to be 1 solar. In the “Model 4”, we fixed the abundance of less constrained elements (N, O, and S) than the others to be 1 solar. The best-fit parameters for these models are also tabulated in table 2. The results are consistent among all these models except for the “Model 4”, in which the estimate of N_{H} and the abundance values are higher and the χ^2 -fitting is worse than the others with significant residuals in the N–O $K\alpha$ energy range. We therefore consider that this is not an appropriate model, and interpret the spectrum based on the result of the other three models.

In a transient plasma like that characterizing our V458 Vul spectra, electrons and ions may not have reached a collisional ionization equilibrium. For non-equilibrium ionization (NEI) plasmas, low levels of ionization of ions can be seen for the temperature determined from the electron bremsstrahlung emission (e.g., Mewe 1998). As a result, the energies of dominant emission features appear shifted

toward lower energies in X-ray CCD spectra by $\gtrsim 10$ eV, which is detectable by XIS (Miyata et al. 2007; Bamba et al. 2008). The degree of the shifts is parameterized by the ionization parameter $\int_0^t dt' n_e(t')$, where $n_e(t)$ is the electron density as a function of time t . We fitted the XIS spectra using an NEI model (Hamilton et al. 1983; Borkowski et al. 1994; Liedahl et al. 1995; Borkowski et al. 2001) and found a 90% lower limit to the ionization parameter of $1.4 \times 10^{12} \text{ s cm}^{-3}$. Finding a value higher than $\approx 10^{11} - 10^{12} \text{ s cm}^{-3}$ implies that the XIS spectrum is consistent with being at a collisional equilibrium (Mewe 1998).

5. Discussion

5.1. Interstellar and Circumstellar Extinction

From our spectral fitting, we derived a neutral hydrogen column density of $N_{\text{H}} = (1.8 - 4.6) \times 10^{21} \text{ cm}^{-2}$ along the line of sight to V458 Vul (table 2). The value is consistent with the interstellar extinction estimated by Poggiani (2008). By the time of the Suzaku observation, the color index ($B - V$) of the nova has plateaued from the initial redder values. Therefore, most of the observed extinction stems from the interstellar medium, not from the material local to the nova.

The average interstellar hydrogen density ($n_{\text{H,ISM}}$) in the line of sight is then estimated as $\sim 0.1 \text{ cm}^{-3}$, which is smaller by an order of magnitude than the canonical value of $n_{\text{H,ISM}} = 1 \text{ cm}^{-3}$. We suspect that this is due to the off-plane location of the nova at -3.6 degree in the Galactic latitude (Schlegel et al. 1998).

5.2. Chemical Abundance

5.2.1. Previous Abundance Studies

WDs causing novae can have two different chemical compositions depending on their mass; CO-type for sources less than $\sim 1.2 M_{\odot}$ and ONe-type for those more than $1.1 - 1.2 M_{\odot}$ (Iben & Tutukov 1989). With a less mass, the gravitational potential on the WD surface is smaller and the peak temperature in the thermo-nuclear runaway is lower. Together with a different core composition, the two types of novae yield different species of elements in runaways. The major nuclear reaction in CO novae does not go beyond elements heavier than O, while that in ONe novae reaches up to Si and S. Theoretical calculations show that intermediate-mass species are enhanced in the ejecta from ONe novae (Starrfield et al. 2008; Jose & Hernanz 1998; José & Hernanz 2007). Also, the ratio of C and N against O increases as the WD mass increases (Jose & Hernanz 1998; José & Hernanz 2007). The chemical pattern of nova ejecta thus provides important clues to guess the type of the WD that hosts the nova.

Three novae have been studied to discuss the chemical abundance in their hard X-ray plasma. V382 Vel was observed by medium-resolution gas scintillation proportional counters aboard BeppoSAX on day 15 (Orio et al. 2001) and by a high-resolution grating spectrometer aboard Chandra on day 268, after the nova had

Table 2. Best-fits spectral parameters.

Param.	Unit	Model 1* [†]	Model 2* [†]	Model 3* [†]	Model 4* [†]
N_{H}	10^{21} (cm ⁻²)	2.8 (1.8–4.6)	2.8 (1.8–4.4)	2.8 (1.9–4.1)	3.8 (2.9–4.8)
$k_{\text{B}}T$	(keV)	0.64 (0.57–0.71)	0.65 (0.60–0.71)	0.64 (0.60–0.70)	0.64 (0.59–0.69)
Z_{N}	(solar)	1.0 (0.0–45)	1.3 (0.0–35)	1 (fixed)	1 (fixed)
Z_{O}	(solar)	0.0 (0.0–1.6)	0.0 (0.0–1.1)	0.0 (0.0–0.8)	1 (fixed)
Z_{Ne}	(solar)	0.6 (0.3–1.8)	0.5 (0.3–1.1)	0.6 (0.3–1.2)	1.2 (0.6–1.9)
Z_{Mg}	(solar)	0.4 (0.2–1.3)	0.5 (0.3–1.1)	0.4 (0.2–0.9)	0.9 (0.5–1.4)
Z_{Si}	(solar)	0.5 (0.3–1.3)	0.5 (0.3–1.1)	0.5 (0.3–0.9)	0.9 (0.5–1.5)
Z_{S}	(solar)	0.6 (0.0–1.5)	0.5 (0.3–1.1)	0.6 (0.0–1.3)	1 (fixed)
Z_{Fe}	(solar)	0.2 (0.1–0.8)	0.2 (0.1–0.6)	0.2 (0.1–0.4)	0.5 (0.3–0.7)
Z_{Ni}	(solar)	0.2 (0.1–0.8)	0.2 (0.1–0.6)	0.2 (0.1–0.4)	0.5 (0.3–0.7)
F_{X}^{\ddagger}	10^{-12} (erg s ⁻¹ cm ⁻²)	1.1 (0.5–1.7)	1.1 (0.7–1.5)	1.1 (0.7–1.6)	1.1 (0.8–1.5)
L_{X}^{\S}	10^{34} (erg s ⁻¹)	5.9	5.7	5.9	7.2
$\chi^2/\text{d.o.f.}$		385.2/456	391.0/449	385.3/447	403.3/449

* The statistical uncertainties are indicated by the 90% confidence range.

[†] Fitting with constraints with $Z_{\text{Fe}} = Z_{\text{Ni}}$ (Model 1), $Z_{\text{Fe}} = Z_{\text{Ni}}$ and $Z_{\text{Ne}} = Z_{\text{Mg}} = Z_{\text{Si}} = Z_{\text{S}} = 1$ (Model 2), $Z_{\text{Fe}} = Z_{\text{Ni}}$ and $Z_{\text{N}} = 1$ (Model 3), and $Z_{\text{Fe}} = Z_{\text{Ni}}$ and $Z_{\text{N}} = Z_{\text{O}} = Z_{\text{S}} = 1$ (Model 4).

[‡] The X-ray flux in the 0.3–3.0 keV band.

[§] A distance of 13 kpc is assumed.

turned off (Ness et al. 2005). V4633 Sgr was observed by medium-resolution CCD spectrometers aboard XMM-Newton 2.6 and 3.5 years after the explosion (Hernanz & Sala 2007). RS Oph was observed by high-resolution grating on Chandra and XMM-Newton (Nelson et al. 2008; Drake et al. 2008a; Ness et al. 2008a) ten times from day 14 to day 239.

In the high-resolution grating spectra of the early hard X-rays in RS Oph (Ness et al. 2008a), bremsstrahlung continuum emission and line emission are resolved. N is found overabundant as a fingerprint of the CNO cycle for the H fusion. High N abundances thus point to the ejected material from the WD as the source for the X-ray emission. However, in the specific case of RS Oph, the abundances must be compared to those of the accreted material from its giant companion (thus the composition of the companion) in order to confirm that the observed X-rays originate from the WD ejecta. In a grating spectrum of V382 Vel, a high N abundance was also found (Ness et al. 2005). However, the observation was conducted well after the nova had turned off, thus reflecting the late nebular emission rather than the early hard emission.

In the medium-resolution studies, the chemical pattern is murkier for being unable to derive the abundances element by element. Nevertheless, Orio et al. (2001) found a hint of significant iron depletion in V382 Vel. Hernanz & Sala (2007) tried two thermal models with different chemical patterns to fit the V4633 Sgr spectra, one with all elements fixed to the solar values and the other fixed to those of a CO nova shell. Both models can explain the data.

5.2.2. Abundance of V458 Vul

We observed V458 Vul with the medium-resolution spectrometer aboard Suzaku. A high signal-to-noise ratio spectrum allows us to constrain the abundance of metals individually for seven elements (table 2). The abundance values are subject to change due to the unconstrained He

abundance. He, along with H, contributes to the continuum emission in the observed band. We fixed the He abundance to the solar value in our fitting procedures, but an increased abundance of He leads to an increased estimate of metal abundances. Therefore, the best-fit abundance values of metals should be considered only in a sense relative to each other.

Using the result of the “Model 2”, we define the metal abundance, $Z_{\text{m}} = 0.5 Z_{\odot}$, which we derived by collectively thawing Ne, Mg, Si, and S abundances. With respect to this value, the best-fit parameters of the spectrum shows an enhanced N abundance with $Z_{\text{N}}/Z_{\text{m}} \sim 2.6$ and deficient O and Fe abundances with $Z_{\text{O}}/Z_{\text{m}} \sim 0$ and $Z_{\text{Fe}}/Z_{\text{m}} \sim 0.4$.

We note here that systematic uncertainties can arise from possible inaccurate modeling. First, the uncertainty in the N_{H} estimate amplifies the uncertainty of the N and O abundances, although we consider it unlikely that the both elements have the solar abundance from the result of the “Model 4”. Second, a single temperature model may be an oversimplification. This leads to particularly high uncertainties in elements formed far away from the isothermal temperature. For example, in a 0.65 keV plasma, the lines of S and Si (the peak formation temperature ~ 1.4 keV) have to be formed in the wings of their line emissivity functions. Small changes in temperature require large changes in abundance, because the slope of the line emissivity functions is steeper in their wings than near the peak. This explains the increasing uncertainties of Mg, Si, to S in the “Model 1”. The same arguments apply for the low-temperature lines of N and O (the peak formation temperature ~ 0.3 keV). If the plasma is not isothermal and additional components with temperatures of 0.3 and 1.4 keV are present, significantly lower abundances for N, O, Si, and S will be obtained. Without a knowledge of the true emission measure distribution such as that determined by Ness et al. (2005), it is impossible to determine the accurate abundances. We speculate,

however, that contributions from plasma with temperatures below 0.3 keV and above 1.4 keV are minor, judging from a high ratio of N VII to N VI and a low ratio of Si XIV and Si XIII (figure 3).

With these uncertainties in mind, it is interesting to note that an N enhancement and a Fe deficiency in hard X-ray emission are seen in all novae with a Z_N and a Z_{Fe} measurement, respectively, including the present work (Mukai & Ishida 2001; Orio et al. 2001; Ness et al. 2005; Ness et al. 2008a). We speculate that this typical pattern in the X-ray spectra is a consequence of these novae belonging to the ONe-type. The deficiency of the Fe abundance with respect to the intermediate-mass elements is consistent with the theoretical understanding that ONe-type novae produce elements up to Si and S. The N enhancement can be interpreted as an outcome of the H fusion on the WD surface, where the CNO cycle produces abundant N by the N to O conversion as the rate-determining process. The abundance of N with respect to O increases for more massive ONe-type novae. A quantitative comparison with theoretical work (Starrfield et al. 2008; Jose & Hernanz 1998; José & Hernanz 2007) is hampered by a relatively large uncertainty in our fitting results, but the overall abundance pattern in V458 Vul indicates that this is an ONe-type nova.

5.3. Plasma Origin and Parameter Constraints

We first argue that the X-ray emission observed from V458 Vul is most likely to be the internal shock of the nova ejecta, and not due to other processes. The hard spectrum exceeding 1 keV shows that it is neither the SSS emission nor the reprocessed emission of it. The possible N enhancement is consistent with the plasma mostly composed of the ejecta. Shocks might occur externally between the ejecta and swept-up interstellar matter, but the total mass of the swept-up matter by the time of the Suzaku observation is too small compared to the ejected mass. The ejecta mass is estimated to be in the range of $\sim 10^{-3}$ – $10^{-6} M_\odot$ (Gehrz et al. 1998), whereas the swept-up mass is $\sim 4\pi/3(v_0 t_S)^3 m_p n_{H,ISM} \sim 10^{-11} M_\odot$ where m_p is the proton mass, $n_{H,ISM} = 1 \text{ cm}^{-3}$ is the ISM density, $v_0 = 1.8 \times 10^3 \text{ km s}^{-1}$ is the initial speed of expanding shell (Buil & Fujii 2007), and t_S is the time of the Suzaku observation elapsed from the explosion. If we adopt $n_{H,ISM} = 155 \text{ cm}^{-3}$, the densest value in the surrounding planetary nebula (Wesson et al. 2008), the swept-up mass is far smaller than the typical ejecta mass.

In the case of symbiotic novae like RS Oph, early hard emission can be produced by external shocks between the expanding ejecta and the stellar wind of the giant companion (Bode et al. 2006). This does not work for classical novae, in which the secondary is a main sequence star and the stellar wind is not dense enough (O’Brien et al. 1994). While no observational evidence exists that V458 Vul is not a symbiotic nova, shock emission by collisions between the expanding ejecta and the stellar wind of the companion is not likely. In RS Oph, the shock itself occurred over a relatively short time scales, and the hard X-ray emission quickly faded afterwards (Bode et al. 2006), while the X-

ray count rate in V458 Vul rises with no indication of a decline. It is most likely that the X-rays from V458 Vul originate in shocks internal to the expanding system, presumably between slower and earlier pre-maximum ejecta and faster and later nova winds (Friedjung 1987; Mukai & Ishida 2001). However, in the later Swift observations one year after the nova, this hard X-ray emission still remains and exhibits highly variable flux in anti-correlation with the UV flux (Ness et al. 2008b). Elaborated theoretical work is necessary to explain all these properties to see if the internal shock interpretation is valid.

From the spectral fits, the absorption-corrected X-ray luminosity at the Suzaku observation is $L_X(t_S) = 6 \times 10^{34} \text{ erg s}^{-1}$ in the 0.3–3.0 keV band at an assumed distance of 13 kpc. The luminosity is in a typical range for classical novae (Mukai et al. 2008). The X-ray volume emission measure at the same time is $EM(t_S) = n_e^2(t_S)V_X(t_S) \sim 7 \times 10^{57} \text{ cm}^{-3}$, where $V_X(t)$ and $n_e(t)$ represent the X-ray-emitting volume and the plasma density as a function of time t .

With these measurements and several simplifying assumptions, a crude estimate can be obtained for the lower and upper bounds of the plasma density at t_S . Assuming that the plasma density is uniform and that the expansion velocity v_0 has not changed since the outburst, the X-ray emitting volume cannot exceed the volume of the expanding shell; i.e., $V_X(t_S) < 4\pi/3(v_0 t_S)^3$. The observed $EM(t_S)$ thus implies that the density must be $n_e(t_S) > 8 \times 10^5 \text{ cm}^{-3}$. If we further assume that the plasma was created at one epoch and not heated repeatedly, the plasma density cannot be too high to cool radiatively too soon. The cooling time t_{rc} at t_S is approximated as $3n_e(t_S)k_B T(t_S)V_X(t_S)/L_X(t_S)$. With $t_{rc} > 100$ day, which is an approximate duration of the detected X-ray coverage by Swift, the upper bound is estimated as $n_e(t_S) < 4 \times 10^7 \text{ cm}^{-3}$. The lower and upper bounds put $n_e(t_S)$ within a range of two orders around $\approx 10^6 \text{ cm}^{-3}$. Orio et al. (1996) derived a similar density of $n_e \sim 2 \times 10^6 \text{ cm}^{-3}$ assuming $V_X(t) = 4\pi/3(v_0 t)^3$ for V351 Pup observed 16 month after its explosion.

6. Summary

The classical nova V458 Vul was discovered on 2007 August 8. In response to the Swift detection of X-ray emission on day 70, we conducted a target of opportunity observation on day 88 with Suzaku.

The X-ray spectrum obtained by the XIS is attributable to a single-temperature (~ 0.64 keV) optically-thin thermal plasma emission at a collisional equilibrium with an interstellar extinction of $\sim 3 \times 10^{21} \text{ cm}^{-2}$. In addition to the plasma temperature and the amount of extinction, the chemical abundances of conspicuous elements were derived. The abundance pattern is characterized by a possible enhancement of N and deficiencies of O and Fe abundances with respect to other metals. From the X-ray luminosity of $6 \times 10^{34} \text{ erg s}^{-1}$, the plasma temperature of 0.64 keV, and the volume emission measure of $7 \times 10^{57} \text{ cm}^{-3}$ at the time of the Suzaku observation, we

constrained the average plasma density to be $8 \times 10^5 - 4 \times 10^7 \text{ cm}^{-3}$ assuming a constant expansion velocity of $1.8 \times 10^3 \text{ km s}^{-1}$. All the observed X-ray properties obtained by Suzaku can be interpreted as the emission arising from shocks of ejecta in a nova at a ~ 13 kpc distance.

We demonstrated the capability of the XIS to yield a high signal-to-noise ratio spectrum for a moderately bright X-ray nova in a reasonable telescope time. This put constraints on physical values and chemical compositions of the X-ray emission. In conjunction with monitoring observations routinely done by Swift, we anticipate that similar Suzaku observations can be executed for several novae every year.

The authors appreciate an excellent review by Gloria Sala. We also thank Kazuhiro Nakajima and Hitoshi Yamaoka in the Variable Star Observers League in Japan for providing optical data of V458 Vul, and the Suzaku telescope managers for allocating a part of the director's discretionary time for this observation. Support for this work was provided by the National Aeronautics and Space Administration through Chandra Postdoctoral Fellowship Awards Number PF6-70044 (M.T.) and PF5-60039 (J.-U.N.) issued by the Chandra X-ray Observatory Center, which is operated by the Smithsonian Astrophysical Observatory for and on behalf of the National Aeronautics Space Administration under contract NAS8-03060. J.J.D. was supported by NASA contract NAS8-39073 to the CXC during the course of this research. D.T. is financially supported by the Japan Society for the Promotion of Science. This research has made use of the SIMBAD database operated at CDS, Strasbourg, France and the NASA/IPAC Extragalactic Database (NED) which is operated by the Jet Propulsion Laboratory, California Institute of Technology, under contract with the National Aeronautics and Space Administration.

References

- Anders, E. & Grevesse, N. 1989, *Geochim. Cosmochim. Acta*, 53, 197
- Bamba, A., et al. 2008, *PASJ*, 60, 153
- Bianciardi, G., Villegas, J. M., & Sanchez, A. 2007a, *Central Bureau Electronic Telegrams*, 1035, 2
- Bianciardi, G., Puig, X., & Forne, E. 2007b, *Central Bureau Electronic Telegrams*, 1038, 2
- Bode, M. F., et al. 2006, *ApJ*, 652, 629
- Borkowski, K. J., Sarazin, C. L., & Blondin, J. M. 1994, *ApJ*, 429, 710
- Borkowski, K. J., Lyerly, W. J., & Reynolds, S. P. 2001, *ApJ*, 548, 820
- Broens, E., Hornoch, K., Cloesen, P., van Loo, F., Diepvens, A., Hautecler, H., Lehky, M., & Muyliaert, E. 2007, *IAU Circ.*, 8878, 2
- Buil, C. & Fujii, M. 2007, *IAU Circ.*, 8862, 2
- Burrows, D. N., et al. 2005, *Space Science Reviews*, 120, 165
- Casas, R., Fernandez-Ocana, M. A., Diepvens, A., Scarmato, T., & Lehky, M. 2007, *Central Bureau Electronic Telegrams*, 1035, 3
- Dickey, J. M., & Lockman, F. J. 1990, *ARA&A*, 28, 215
- Downes, R. A., & Duerbeck, H. W. 2000, *AJ*, 120, 2007
- Drake, J. J., et al. 2007, *The Astronomer's Telegram*, 1246, 1
- Drake, J. J., Laming, M., Ness, J.-U., & Starrfield, S. 2008a, *ApJ*, submitted
- Drake, J. J., et al. 2008b, *The Astronomer's Telegram*, 1631, 1
- Friedjung, M. 1987, *A&A*, 180, 155
- Gehrz, R. D., Truran, J. W., Williams, R. E., & Starrfield, S. 1998, *PASP*, 110, 3
- Hamilton, A. J. S., Chevalier, R. A., & Sarazin, C. L. 1983, *ApJS*, 51, 115
- Hernanz, M., & Sala, G. 2002, *Science*, 298, 393
- Hernanz, M. & Sala, G. 2007, *ApJ*, 664, 467
- Hyodo, Y., Tsujimoto, M., Hamaguchi, K., Koyama, K., Kitamoto, S., Maeda, Y., Tsuboi, Y., & Ezoe, Y. 2008, *PASJ*, 60, 85
- Iben, I. J., & Tutukov, A. V. 1989, *ApJ*, 342, 430
- Ishisaki, Y., et al. 2007, *PASJ*, 59, S113
- Jose, J., & Hernanz, M. 1998, *ApJ*, 494, 680
- José, J & Hernanz, M. 2007, *J. Phys. G: Nucl. Part. Phys.*, 34, R431
- Kalberla, P. M. W., Burton, W. B., Hartmann, D., Arnal, E. M., Bajaja, E., Morras, R., Pöppel, W. G. L. 2005, *A&A*, 440, 775
- Kiss, L. & Sarneckzy, K. 2007, *Central Bureau Electronic Telegrams*, 1038, 1
- Kokubun, M., et al. 2007, *PASJ*, 59, S53
- Koyama, K., et al. 2007, *PASJ*, 59, S23
- Krautter, J. 2002, *Classical Nova Explosions*, 637, 345
- Labordena, C., Forne, E., & Ardanuy, A. 2007, *IAU Circ.*, 8863, 3
- Liedahl, D. A., Osterheld, A. L., & Goldstein, W. H. 1995, *ApJL*, 438, L115
- Lloyd, H. M., O'Brien, T. J., Bode, M. F., Predehl, P., Schmitt, J. H. M. M., Truemper, J., Watson, M. G., & Pounds, K. A. 1992, *Nature*, 356, 222
- Lynch, D. K., Russell, R. W., Rudy, R. J., & Woodward, C. E. 2007, *IAU Circ.*, 8883, 1
- Mitsuda, K., et al. 2007, *PASJ*, 59, S1
- Mewe, R. 1998, in *Lecture Notes in Physics* vol. 520, ed. J. van Paradijs, & J. A. M. Bleeker (Berlin: Springer-Verlag), 109
- Miyata, E., Katsuda, S., Tsunemi, H., Hughes, J. P., Kokubun, M., & Porter, F. S. 2007, *PASJ*, 59, 163
- Monet, D., et al. 1998, *The PMM USNO-A2.0 Catalog. (1998)*
- Mukai, K. & Ishida, M. 2001, *ApJ*, 551, 1024
- Mukai, K., Orio, M., & Della Valle, M. 2008, *ApJ*, 677, 1248
- Munari, U., Moretti, S., & Tomaselli, S. 2007, *Central Bureau Electronic Telegrams*, 1029, 1
- Nakamura, Y., Yamaoka, H., Dillon, W. G., Guido, E., Sostero, G., Abe, H., Nakano, S., & Labordena, C. 2007, *Central Bureau Electronic Telegrams*, 1029, 2
- Nakano, S., Kadota, K., Waagen, E., Swierczynski, S., Komorous, M., King, R., & Bortle, J. 2007, *IAU Circ.*, 8861, 2
- Nelson, T., Orio, M., Cassinelli, J. P., Still, M., Leibowitz, E., & Mucciarelli, P. 2008, *ApJ*, 673, 1067
- Ness, J.-U., et al. 2003, *ApJL*, 594, L127
- Ness, J.-U., Starrfield, S., Jordan, C., Krautter, J., & Schmitt, J. H. M. M. 2005, *MNRAS*, 364, 1015
- Ness, J.-U., Schwarz, G. J., Retter, A., Starrfield, S., Schmitt, J. H. M. M., Gehrels, N., Burrows, D., & Osborne, J. P. 2007, *ApJ*, 663, 505
- Ness, J.-U., et al. 2008a, submitted to *AJ*

- Ness, J.-U., et al. 2008b, submitted to ApJ
- O'Brien, T. J., Lloyd, H. M., & Bode, M. F. 1994, MNRAS, 271, 155
- Orio, M., Balman, S., della Valle, M., Gallagher, J., & Oegelman, H. 1996, ApJ, 466, 410
- Orio, M., Covington, J., Oegelman, H. 2001, A&A, 373, 542
- Payne-Gaposchkin, C. 1957, The Galactic Novae, (Amsterdam, North Holland)
- Poggiani, R. 2008, Ap&SS, 77
- Prater, T. R., Rudy, R. J., Lynch, D. K., Mazuk, S., Perry, R. B., & Puetter, R. C. 2007, IAU Circ., 8904, 2
- Predehl, P. & Schmitt, J. H. M. M. 1995, A&A, 293, 889
- Samus, N. N. 2007, IAU Circ., 8863, 2
- Scarmato, T. 2007, Central Bureau Electronic Telegrams, 1038, 3
- Schlegel, D. J., Finkbeiner, D. P., & Davis, M. 1998, ApJ, 500, 525
- Serlemitsos, P. J., et al. 2007, PASJ, 59, S9
- Skoda, P., Kubat, J., Votruba, V., Slechta, M., Podskalsky, Z., & Kartak, M. 2007, Central Bureau Electronic Telegrams, 1035, 1
- Smith, R. K., Brickhouse, N. S., Liedahl, D. A., & Raymond, J. C. 2001, ApJ, 556, L91
- Starrfield, S., Truran, J. W., Wiescher, M. C., & Sparks, W. M. 1998, MNRAS, 296, 502
- Starrfield, S., Illiadis, C., Hix, W. R. 2008, in Classical Novae, ed. M. Bode and A. Evans (Cambridge: Cambridge University Press), 77
- Takahashi, T., et al. 2007, PASJ, 59, S35
- Tarasova, T. N. 2007, Informational Bulletin on Variable Stars, 5807, 1
- Wesson, R. et al. 2008, ApJL, in press
- Williams, R. E. 1992, AJ, 104, 725
- Wilms, J., Allen, A., & McCray, R. 2000, ApJ, 542, 914